Quantization effects in ZnO accumulation layers in contact with an electrolyte

D. Eger and Y. Goldstein
The Racah Institute of Physics, The Hebrew University of Jerusalem, 91000 Israel
(Received 2 June 1977)

Accumulation layers with excess surface-electron concentration ΔN of 10^{14} cm^{-2} were produced on ZnO surfaces in contact with an electrolyte. Measurements of ΔN as a function of the surface potential barrier are presented, as well as detailed results of self-consistent quantum calculations. The self-consistent calculations were carried out on the basis of the effective-mass approximation. They take into account the exchange interaction and the penetration of the surface-electron wave functions into the electrolyte. The agreement between theory and experiment is reasonably good.

I. INTRODUCTION

During the last years considerable attention was paid to the so-called "quasi-two-dimensional electronic systems." Most of these systems consisted of quantized inversion layers on silicon surfaces based on metal-oxide-semiconductor (MOS) structures. The highest carrier density obtained on such surfaces approached 10^{13} cm^{-2}. Using the semiconductor-electrolyte system, we succeeded to produce on the ZnO surface extremely strong accumulation layers, having electron surface concentrations ΔN up to 10^{14} cm^{-2}. These are by far the highest densities obtained on any semiconductor. Such strong accumulation layers are characterized by a width of the order of 10 Å and a nearly metallic volume concentration (10^{20} –10^{21} cm^{-3}). Our measurements yield directly the variation of ΔN with the potential barrier height V_s at the ZnO surface.

Some of our preliminary results were already published.[1,2] The experimental results were compared to numerical self-consistent calculations which were obtained by us using the simple Hartree method. It turns out, however, that for our strong accumulation layers, exchange effects are no longer negligible. In addition, for such narrow layers the finite penetration of the electronic wave function into the electrolyte has to be taken into account as well. In this paper we present detailed and improved experimental and theoretical results.

II. EXPERIMENTAL

The formation of a space-charge layer at a semiconductor surface in contact with an electrolyte is based on the blocking characteristics of the interface which prevent charge flow between the two phases.[3,4] In an n-type semiconductor, such blocking usually occurs when the electrolyte is biased negatively with respect to the semiconductor, for which polarity a depletion layer (Schottky barrier) is formed. In some cases, however, there is sufficient blocking even when the electrolyte is biased positively, and it is in this manner that strong accumulation layers could be produced on the ZnO surface.[1,2] Essentially, the equivalent circuit representing the interface can be described as a parallel combination of the space charge capacitance C_s and a leak resistance R_L, both being bias dependent. R_L decreases rapidly with increasing bias and it is for this reason that accumulation layers of ΔN higher than 10^{13} cm^{-2} cannot be maintained in practice under dc operation.[5] In addition, prolonged application of the dc bias produces surface damage by electrochemical processes. The use of pulse techniques developed by us, on the other hand, permits the attainment of much stronger accumulation layers and, at the same time, minimizes surface damage.

The measurements were carried out in semiconducting ZnO samples of 10–20 Ω cm resistivity, using the "oxygen" $(000\bar{1})$ surface. The samples were mechanically polished to a flatness of 1 μ and subsequently chemically etched. Usually the etchant used was concentrated HCl which yielded excellent blocking characteristics. Some other etchants like H_3PO_4 were also tried, with similar results. Curiously enough, we were unable to obtain blocking characteristics on the "zinc" (0001) face and this surface was not investigated.

The cell used consisted of a platinum electrode, the ZnO sample under study, and a reference electrode (Ag-AgCl) close to the ZnO surface. The electrolyte was generally KCl (2N), but other electrolytes such as NaCl, $CuSO_4$, $NaHCO_3$, and KBr gave similar results. The area of the ZnO surface exposed to the electrolyte was about 0.1 cm^2, while the rest of the sample and Ohmic contact were well insulated from the solution.

A current pulse of constant amplitude was applied across the Pt and the ZnO electrodes, and the voltage developed between the reference electrode and the ZnO bulk was displayed on a cathode-ray

oscilloscope (CRO). This voltage represents to a very good approximation[3,5] the change $\delta V_s = V_s - V_{s0}$ in barrier height V_s at the ZnO space-charge layer formed (V_{s0} being the initial barrier height). Since the charging current is constant, the time axis is directly proportional to the change $\delta Q_s = Q_s - Q_{s0}$ in the space-charge density at the ZnO surface. Hence, the CRO trace so obtained yields directly the entire δQ_s vs δV_s curve. The only requirement is that the leak current (through R_L) be negligible compared to the charging current. This can be achieved by making the charging current sufficiently large so that the charging time (the pulse duration) becomes small compared to $R_L C_s$.

In depletion layers (electrolyte negative with respect to ZnO) there is execellent blocking so that R_L is very high (~10^8 Ω) and the above requirement is easily satisfied. In accumulation layers (electrolyte positive), on the other hand, R_L decreases with increasing applied voltage and care has to be taken to ensure that there is no appreciable leakage current.

In order to measure the leakage current I_L and ensure that it does not affect our results, we varied the time required to charge the space-charge capacitance C_s. This was achieved by performing measurements using current pulses of different amplitudes. Typical charging times ranged between 10 and 100 μsec. As the current pulse is applied the reference electrode potential δV_s increases as a function of time t due to the charging of the space-charge capacitance C_s. As long as I_L is negligible compared to the charging current I_c, the time axis is proportional to the change in the space charge, $\delta Q_s = I_c t$. However, as V_s increases with time (in accumulation layers), R_L decreases and thus I_L increases and becomes comparable to I_c. Now the δV_s vs t curve starts to deviate from δV_s vs δQ_s curve; δV_s increases more slowly and eventually reaches a steady value. Since this steady value $\delta V_{s\infty}$ corresponds to $I_L = I_c$, the leakage resistance can be calculated from $R_L = \delta V_{s\infty}/I_c$. If we repeat the measurement using a higher value of the charging current I_c, the δV_s vs t curve will start deviating from the δV_s vs δQ_s curve at a higher voltage. This is illustrated in Fig. 1, where a series of curves of δV_s in accumulation layer is plotted as a function of the charge $Q = I_c t$ (in units of the electronic charge e). The different curves correspond to different charging currents I_c. As can be seen, as I_c becomes larger, the deviation from the true δV_s vs δQ_s curve occurs at a higher δV_s value. Obviously, that part of the curve where two measurements at different currents coincide represents the true δV_s vs δQ_s curve.

A complete δQ_s vs δV_s curve is shown in Fig. 2. Here δQ_s is expressed in terms of the change δN

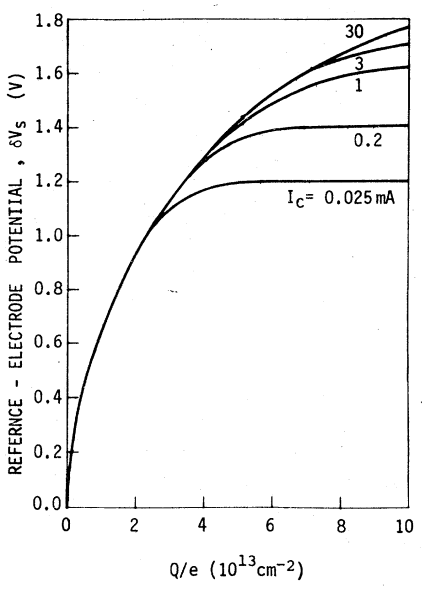

FIG. 1. Reference electrode potential δV_s as a function of the charge $Q = I_c t$ in units of the electronic charge e. Different curves correspond to different charging currents I_c as denoted in the figure.

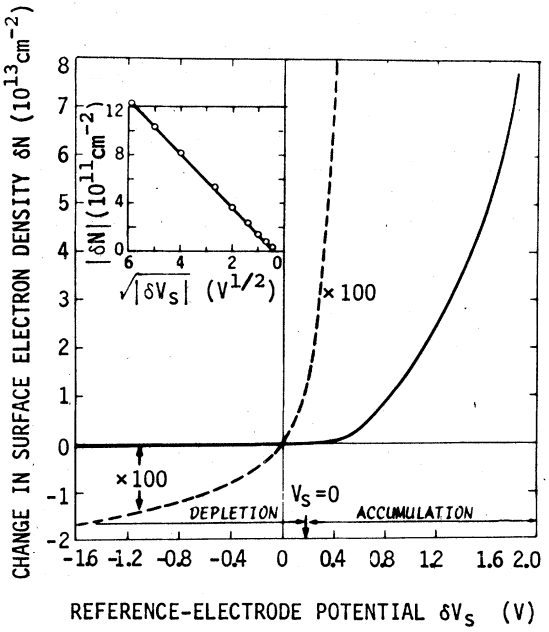

FIG. 2. Change δN in the surface-electron density as a function of the reference electrode potential δV_s for accumulation and depletion layers (full line). The position of "flat bands" ($V_s = 0$) is shown by the arrow. The dashed curve is a hundredfold expansion of the depletion layer and weak accumulation layer data. In the insert the data at large negative values of V_s (depletion layer) are plotted as a function of $|\delta V_s|^{1/2}$ for determining V_{s0}.

$= \Delta N - \Delta N_0 (= \delta Q_s/e)$ in the surface-electron density. As will be discussed in a moment, the initial condition of the surface on this sample, (with no pulse applied) was characterized by $V_{s0} = -0.18$ V and $\Delta N_0 = -10^{11}$ cm^{-2} (weak depletion layer). Thus, flat-band conditions ($V_s = 0$) are reached when $\delta V_s = +0.18$ V. For higher positive δV_s values, an accumulation layer is formed and, as expected,[6] δN increases very rapidly with δV_s. In the reverse polarity, the weak depletion layer present initially is being enhanced. In this range $|\delta N|$ is small and varies slowly with δV_s. The δN scale has been expanded a hundredfold (dashed curve) in order to display this variation. Extension of the measurements to large negative values of δV_s (see insert in Fig. 2) was used to determine V_{s0} and ΔN_0. This is a standard and well-known procedure based on the fact[5,6] that in depletion layers ΔN is given approximately by

$$|\Delta N| \approx A |V_s|^{1/2} .$$

For large values of $|\delta V_s|$,

$$|\delta N| \approx A(|\delta V_s|^{1/2} - |V_{s0}|^{1/2}) .$$

Thus the intercept at $\delta N = 0$ of the straight line at large $|\delta V_s|$ yields V_{s0}. Using these initial conditions, one can plot ΔN as a function of V_s, with the reference point now being flat-band conditions. The initial condition of the ZnO surface was always found to correspond to a weak depletion layer, with V_{s0} ranging between -0.1 to -0.3 volts.

As explained above, one can derive the leakage resistance R_L from the steady value of the voltage $\delta V_{s\infty}$ (see Fig. 1). In Fig. 3, R_L is plotted (on a logarithmic scale) as a function of the barrier

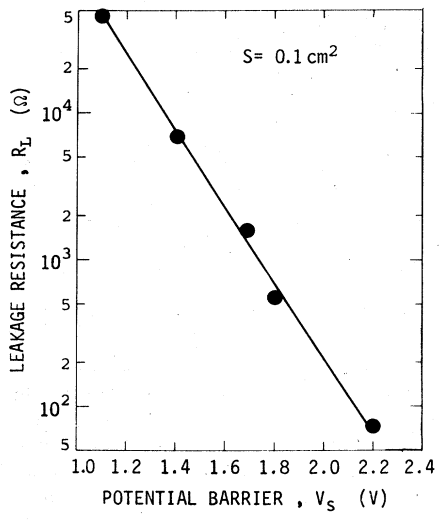

FIG. 3. Semilogarithmic plot of the leakage resistance R_L as a function of the potential barrier V_s.

height V_s in accumulation layer. As can be seen the leakage resistance decreases exponentially with V_s. However, this decrease is slow enough to enable measurements up to about $\Delta N \approx 10^{14}$ cm^{-2}.

III. THEORY

A theoretical derivation of the ΔN vs V_s curve requires a self-consistent solution of Schrödinger's and Poisson's equations. This kind of calculations were made by many authors[7-9] but none of them could be applied to ZnO because of the different band-structure parameters and dielectric constant. Also, no calculations are available for the ΔN range of 10^{13}–10^{14} cm^{-2} encountered for the first time in ZnO. Therefore, the self-consistent calculations had to be carried out anew. We follow Stern[7] in using the effective-mass approximation and characterize the electrons in the accumulation layer by an envelope function

$$\psi_{ik}(x, y, z) = \zeta_i(z) \exp(i \vec{k} \cdot \vec{R}) , \qquad (1)$$

where $\vec{R}$ is the two-dimensional position vector in the plane of the interface, $\vec{k}$ is the two-dimensional wave vector for motion parallel to the interface, z is the distance from the interface into the ZnO, and i denotes the particular subband. The wave functions $\zeta_i(z)$ satisfy the one-dimensional Schrödinger's equation

$$\frac{\hbar^2}{2m^*} \frac{d^2\zeta_i}{dz^2} + [E_i^0 - eV(z)]\zeta_i(z) = 0 . \qquad (2)$$

Here e is the electronic charge, $V(z)$ is the potential in the space-charge region, and the eigenvalue E_i^0 is the bottom level of the ith subband. The effective mass m^* is taken[10] as $0.25 m_e$ and isotropic, where m_e is the free-electron mass. Each subband contains a continuum of levels, due to the variation of the two-dimensional wave vector $\vec{k}$:

$$E_{ik}^0 = E_i^0 + \hbar^2 k^2 / 2m^* . \qquad (3)$$

The boundary conditions usually used[11] in this kind of calculation are $\zeta_i(0) = 0$ and $\zeta_i(\infty) = 0$. The first equation implies an infinite potential barrier at the interface and neglects the penetration of the wave functions into the dielectric. However, as was already pointed out by Stern[11] for similar circumstances, one cannot neglect the penetration of the wave function into the electrolyte, especially for the extremely high surface densities encountered here. This penetration was first included in the calculations by Duke.[8] For Si inversion layers it was shown by Laur and Jayadevaiah,[12] using approximate (Airy) functions, that this penetration is of the order of a few angstroms. To take it into account we proceeded similarly to

these workers. In the electrolyte ($z<0$), we assumed an exponentially decreasing wave function $A\exp(\kappa_i z)$ where $\kappa_i=[2m_e(E_b-E_i^0)]^{1/2}/\hbar$, E_b is the potential barrier in the electrolyte, and m_e is the free-electron mass. As the boundary condition we took the continuity of the logarithmic derivative at the interface $z=0$

$$\left[\left(\frac{d\zeta_i}{dz}\right)/\zeta_i(z)\right]_{z=0}=\kappa_i. \tag{4}$$

After performing the calculations it was pointed out to us that because of the variation of the effective mass between the two materials we should have used the boundary condition given by Daniel and Duke[8] instead of Eq. (4). However, it turns out that E_i^0 is not sensitive to the exact value of κ_i within reasonable limits. We varied E_b between 3–5 eV with almost no effect. Thus we feel that the change of the boundary condition would not affect the results by more than a few percent. Since neither the exact value of E_b nor the effective mass in the electrolyte are known anyhow, we did not see any point in repeating the calculations with a different boundary condition.

The potential $V(z)$ in the space-charge region is found from Poisson's equation

$$\frac{d^2V}{dz^2}=\frac{-\rho(z)}{\epsilon_{sc}\epsilon_0}, \tag{5}$$

where ρ is the charge density, ϵ_0 the permitivity of free space, and ϵ_{sc} the relative dielectric constant in ZnO whose value[13] was taken as 8.5. The variation of the potential in the electrolyte was neglected. The boundary conditions for V are $V(0)=0$, i.e., the energy is measured from the bottom of the conduction band at the interface, and

$$\left.\frac{dV}{dz}\right|_{z=0}=\frac{e\Delta N}{\epsilon_{sc}\epsilon_0}. \tag{6}$$

In calculating the charge density $\rho(z)$ we took into account only the negative charge of the electrons in the accumulation layer and neglected the contribution of the fixed impurity charges. This is an excellent approximation for strong accumulation layers ($\Delta N\gtrsim 10^{12}$ cm^{-2}). Thus,

$$\rho(z)=e\sum_{ik}|\psi_{ik}|^2/\{1+\exp[(E_{ik}^0-E_F)/k_BT]\}, \tag{7}$$

where E_F is the Fermi level and k_B Boltzmann's constant. Performing the summation (integration) on k in Eq. (7) one obtains

$$\rho(z)=e\sum_i N_i\zeta_i^2(z), \tag{8}$$

where the occupation number N_i of the ith sublevel is given by

$$N_i=(k_BT/\pi\hbar^2)m^*\ln\{1+\exp[(E_F-E_{ik}^0)/k_BT]\}. \tag{9}$$

The Fermi level is calculated from the requirement that the integrated charge density equals $e\Delta N$. The integration of Eq. (8) yields

$$\Delta N=\sum_i N_i, \tag{10}$$

which through the E_F dependence of N_i [Eq. (9)] serves for determining E_F.

In the simple Hartree method these are the coupled equations to be solved. The most straightforward method[14] of solution is to apply successive approximations in the numerical computations. One starts with a trial potential $V(z)$ and derives from Schrödinger's equation the energy levels and wave functions. The electron-occupation of the various subbands and hence the space-charge density $\rho(z)$ are then calculated by the use of Fermi-Dirac statistics. The new potential obtained with this charge distribution from Poisson's equation is fed back to the next cycle of the successive approximation. The cycles are repeated until self-consistent solutions are obtained.

In the above calculations we did not take into account the exchange and correlation energies. The correlation energy for a quantized space-charge layer was calculated mainly for Si inversion layers.[15,16] The correction is important for low values of $\Delta N(\simeq 10^{12}$ cm$^{-2})$. In this range of ΔN, however, the zero-temperature ($T=0$) approximation used in the calculations is not valid for our system. Estimation of the correlation energy for finite temperature would be difficult and probably give a lower value then that obtained for $T=0$. As the density of the electrons is increased the correlation energy becomes less significant. For ΔN in the range 10^{13} to 10^{14} cm^{-2} (which is the range we are interested in) the correlation energy was estimated using different approximations given by Jonson[15] and found to change between millielectron volts to tens of millielectron volts. Since these values are much lower than the corresponding $|eV_s|$ values we have omitted the correlation energy from our calculations. The exchange energy, on the other hand, is of the order of 100 meV (see below) and cannot be neglected. In order to correct for the exchange interaction, we add, following Stern,[17] to the energy the term

$$X_{ik}=\sum_{k',j}\int\int\psi_{jk'}^*(\vec{r})\psi_{ik}^*(\vec{r}')V(\vec{r},\vec{r}')\times\psi_{jk'}(\vec{r}')\psi_{ik}(\vec{r})\,d^3r\,d^3r'. \tag{11}$$

Here the summation is over all the occupied states, $V(\vec{r},\vec{r}')$ is given by

$$V(r,r') = -\frac{e^2}{4\pi\epsilon_{sc}\epsilon_0}\left(\frac{1}{[(\vec{R}-\vec{R}')^2+(z-z')^2]^{1/2}} + \frac{\delta}{[(\vec{R}-\vec{R}')^2+(z+z')^2]^{1/2}}\right), \tag{12}$$

$\delta = (\epsilon_{sc}-\epsilon_{el})/(\epsilon_{sc}+\epsilon_{el})$, and ϵ_{el} is the relative dielectric constant of the electrolyte (water). The second term in Eq. (12) arises from the image charge induced in the electrolyte. To evaluate the integral in Eq. (11) we proceed somewhat differently from Stern.[17] We perform the integration in Eq. (11) over the coordinates $\vec{R}$ and $\vec{R}'$ parallel to the interface and change the sum over k' into an integral. After somewhat lengthy calculations we obtain

$$X_{ik} = -(e^2/4\pi\epsilon_{sc}\epsilon_0)\int\int \sum_j \zeta_i(z)\zeta_i(z')\zeta_j(z)\zeta_j(z')[D_j(|z-z'|,k)+\delta D_j(|z+z'|,k)]\,dz\,dz', \tag{13}$$

where

$$D_j(z,k) = \int \exp(-z|\vec{k}'-\vec{k}|) \times \Theta(k'-k_{jF})\,d^2k'/2\pi|\vec{k}'-\vec{k}|. \tag{14}$$

Here $k_{jF} = (2\pi N_j)^{1/2}$ is the Fermi wave number for the jth subband and the Θ function is unity for $k' \leq k_{jF}$ and zero otherwise. The use of the Θ function is valid exactly for $T=0$ while for $T>0$ it constitutes a very good approximation for strong accumulation layers in which $E_F - E_i^0$ is at least several k_BT. Actually, this condition is always satisfied for the first subband and to a lesser extent for the second subband. However, as we shall see below, over 80% of the electrons are in the first subband and almost all the rest in the second subband. Thus, the higher subbands in which this condition is not satisfied are of no interest.

The function D_j can be expressed analytically only for $k=0$

$$D_j(z,0) = [1-\exp(-zk_{jF})]/z. \tag{15}$$

For $k \neq 0$ we expand D_j into a Taylor series and because of the weak dependence of D_j on k retain only the first two terms. From symmetry considerations it is easy to see that the first derivative of D_j is zero. The second derivative $\partial^2 D_j/\partial k^2$, is obtained by first performing the integration in Eq. (14) over the absolute value $|\vec{k}'-\vec{k}|$. The resulting integral is a regular function of k in the vicinity of $k=0$ and we can carry out the differentiation within the integral. Next we set $k=0$ and integrate over the angle of $\vec{k}'$. The result can readily be shown to be

$$\left.\frac{\partial^2 D_j}{\partial k^2}\right|_{k=0} = -\tfrac{1}{2}\left(z+\frac{1}{k_{jF}}\right)\exp(-zk_{jF}). \tag{16}$$

Inserting $D_j(z,0) + \frac{1}{2}k^2(\partial^2 D_j/\partial k^2)_{k=0}$ for $D_j(z,k)$ into Eq. (14) [and (13)] one obtains

$$X_{ik} = X_i + \frac{k^2}{2}\left(\frac{\partial^2 X_{ik}}{\partial k^2}\right)_{k=0}, \tag{17}$$

where X_i is the exchange energy for $k=0$ in the ith subband.

The corrected energy due to exchange interaction can thus be expressed as

$$E_{ik} = E_i^0 + X_i + \frac{\hbar^2}{2m^*}k^2 + \frac{k^2}{2}\left(\frac{\partial^2 X_{ik}}{\partial k^2}\right)_{k=0}. \tag{18}$$

X_i can be viewed as a correction term for E_i^0, the bottom energy of subband i, and we redefine this energy as $E_i = E_i^0 + X_i$. The other term originating from the exchange energy [the last term in Eq. (18)] is proportional to k^2 and can be looked upon as a correction to the kinetic energy. Thus, if we also redefine the effective mass in the ith subband as

$$\frac{1}{m_i^*} = \frac{1}{m^*} + \frac{1}{\hbar^2}\left(\frac{\partial^2 X_{ik}}{\partial k^2}\right)_{k=0}, \tag{19}$$

we can write the energy as

$$E_{ik} = E_i + \hbar^2k^2/2m_i^*. \tag{20}$$

These corrected masses m_i^* were used in calculating the occupation numbers N_i [see Eq. (9)] and the Fermi level E_F.

In order to illustrate how the exchange correction was introduced into the iterative calculation discussed above, we shall describe one cycle of the iteration. The potential $V(z)$ obtained from the previous iteration is fed into a subprogram for integrating Eq. (2). This yields the subband energies E_i^0 and the normalized wave functions $\zeta_i(z)$. Next, we calculate the exchange energy X_i by a numeric two-variable integral and the effective-mass correction $(\partial^2 X_{ik}/\partial k^2)_{k=0}$ [see Eqs. (13)–(17)]. The corrected energies E_i and effective masses m_i^* are inserted into Eq. (9), and Eq. (10) is solved for the Fermi level E_F. The occupation numbers N_i are then calculated from Eq. (9) and the charge

density $\rho(z)$ from Eq. (8). Finally, the new potential $V(z)$ is derived by integrating Poisson's equation, Eq. (5). Usually not the entire new $V(z)$ was used for the next iteration but some average between the new and old one in order to avoid convergence problems.

IV. RESULTS OF CALCULATIONS AND COMPARISON WITH EXPERIMENT

Figure 4 depicts the calculated values of the potential $V(z)$ in the accumulation layer as a function of the distance z from the interface for the case of a very strong accumulation layer ($\Delta N = 5\times10^{13}$ cm^{-2}). As can be seen from the figure, most of the potential drop occurs within 10 Å of the interface. The positions of the bottom edges of the first two subbands are shown by the two full horizontal lines labeled E_0 and E_1 and the Fermi level E_F by the dotted line. The z dependence of the envelope wave functions in these two subbands is shown by the two dashed lines labeled ζ_0 and ζ_1, using the levels E_0 and E_1 as the zero lines for the wave functions. Notice that the wave functions

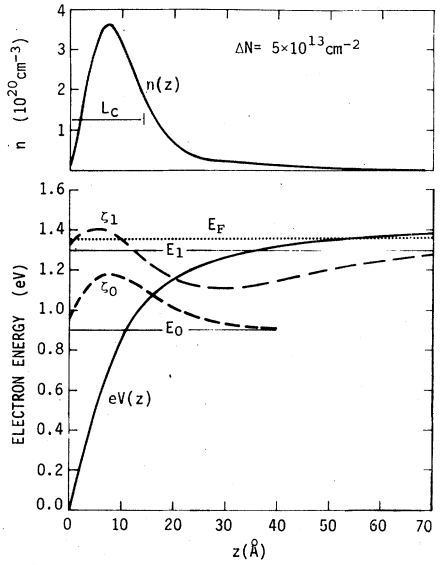

FIG. 4. Calculated values of the potential $V(z)$ in accumulation layer as a function of the distance z from the ZnO-electrolyte interface for a surface-electron concentration of $\Delta N = 5\times10^{13}$ cm^{-2}. The two horizontal lines labeled E_0 and E_1 show the positions of the bottom edges of the first two subbands while the line labeled E_F (dotted) shows the position of the Fermi level. The envelope wave functions in the first two subbands, ζ_0 and ζ_1, are shown by the two dashed lines, using the levels E_0 and E_1 as the zero lines for the wave functions. The upper part of the figure shows $n(z)$ the electron bulk concentration in the space-charge region. The effective-charge distance L_c is also marked in the figure.

start at the ZnO-electrolyte interface ($z=0$) with a finite value. This is due to the assumption of a finite potential barrier in the electrolyte. Because of the penetration of the wave functions into the electrolyte, the maxima of ζ_0 and ζ_1 are displaced by 1–2 Å to the left from their position for an infinite barrier. The displacement affects somewhat the spatial distribution of the electrons in the accumulation layer and brings them closer to the interface. It also lowers to some extent the energies of the subbands (E_0 and E_1). To the right, the wave functions penetrate inside the ZnO bulk relatively far into the "negative kinetic energy" region. This is due to the low effective potential barrier for these states (about 0.5 volts for ζ_0 and 0.1 volts for ζ_1). It should be pointed out, however, that the penetration of the wave functions (in both directions) affects only slightly the electron concentration.

The total electron bulk density $n(z)$ in the accumulation layer (summed over all the subbands) is shown in the upper part of Fig. 4. As can be seen, this density is of the order of 10^{20} cm^{-3}, almost metallic. The maximum of $n(z)$ is between 7 and 8 Å. The density of the electrons that penetrate into the electrolyte is very small, as can be seen by the almost vanishing value of $n(z)$ at $z=0$. The penetration of the wave functions into the ZnO bulk gives rise to a long tail in $n(z)$ towards large z. The amplitude of this tail is small and relatively very few electrons are at appreciable distances from the interface. Most of the excess electrons are within 15 Å of the interface as shown also by the marked value of the effective charge distance L_c. This distance is defined[6] as

$$L_c \equiv \epsilon_{sc}\epsilon_0 \left| V_s / e\Delta N \right| , \tag{21}$$

i.e., L_c is the separation of an equivalent parallel-plate capacitor whose one plate is at the interface and the other inside the ZnO crystal. It is easy to show that L_c is the center of mass of $n(z)$ and thus can be looked upon as the effective width of the accumulation layer.

In Fig. 5 the various calculated energy levels are shown as functions of ΔN, in the accumulation layer. The three solid curves depict the positions of the bottom edges E_0, E_1, and E_2 of the first three subbands, while the dotted line shows the position of the Fermi level E_F. All energy levels are measured from the bottom of the conduction band at the surface. The separation between the energy levels is seen to decrease with decreasing ΔN, as expected. The classical regime is reached when these separations become comparable to $k_B T$($\Delta N \approx 5\times10^{11}$ cm^{-2}). Also shown (dashed curves) are the fractional occupations η_0, η_1, and η_2 of the first three subbands. Over most of the ΔN range dis-

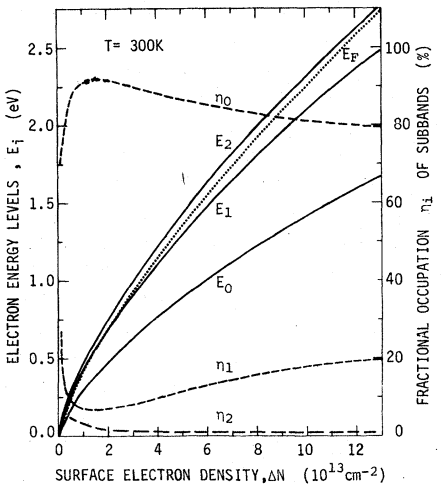

FIG. 5. Calculated values of the bottom edges of the first three subbands, E_0, E_1, and E_2 (full lines) and the Fermi level, E_F (dotted line) as a function of the surface-electron density, ΔN. The fractional occupation of the first three subbands are also shown by the dashed lines labeled η_0, η_1, and η_2.

played, η_0 is over 80% while η_1 is 10–20% and η_2 is less than 1%. Thus the majority of the electrons occupy the first subband so that the accumulation layer can be viewed as a two-dimensional electron gas system (the so-called quantum limit[7]).

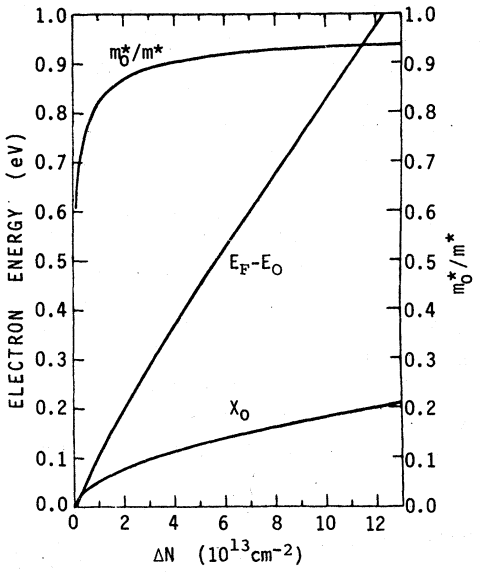

FIG. 6. Position of the Fermi level measured from the bottom of the first subband, $E_F - E_0$, as a function of the surface-electron concentration. The upper line shows the ratio of m_0^*/m^* of the effective mass in the first subband to the uncorrected effective mass (see text). At the bottom of the figure is shown X_0, the value of the exchange energy at $k=0$ for the first subband.

In Fig. 6 is shown the position of the Fermi level, measured from the bottom of the first subband $E_F - E_0$ as a function of ΔN. This dependence is almost linear and the slight curvature is due mainly to the presence of the other subbands. The variation of m_0^*, the effective mass in the first subband, (due to the exchange energy) is shown by the upper line, where the ratio m_0^*/m^* (m^* being the uncorrected effective mass) is plotted against ΔN. The value of the exchange energy at $k=0$ for the first subband X_0 is shown at the bottom of the figure. It is seen that X_0 rises monotonously with ΔN and is close to 0.2 eV at $\Delta N = 10^{14}$ cm^{-2}.

The experimental values of ΔN (full dots and squares) are plotted in Fig. 7 as a function of V_s in the accumulation layer. The squares represent data obtained by the method described above (Fig. 2). With this method it is possible to measure reliably the charging process of the space charge up to about $\Delta N = 5 \times 10^{13}$ cm^{-2}. The dots represent data obtained by a different method which enables the measurements to be extended up to $\Delta N = 10^{14}$ cm^{-2}. This method was developed in our laboratory and will be described shortly in a separate publication.[18] The rising solid curve is the result of the

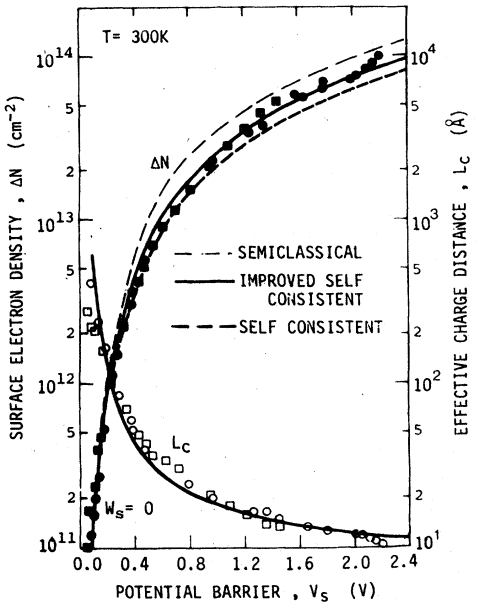

FIG. 7. Experimental values of ΔN as a function of the barrier height V_s in accumulation layer. The full squares and dots represent data obtained with different methods (see text). The calculated ΔN curves shown were obtained using the semiclassical approximation (long-dashed), the previous self-consistent calculation (short-dashed), and the present improved self-consistent calculation (full line). Also shown are the experimental values of the effective-charge distance L_c (empty squares and circles) together with the calculated line.

present self-consistent calculations and agrees very well with experiment. For comparison we also show the results of previous self-consistent calculations[1,2] (short-dashed line), which neglected the exchange interaction and assumed an infinite barrier at the ZnO/electrolyte interface. As can be seen, the difference between the two self-consistent curves is not insignificant at high ΔN values. The long-dashed curve represents the semiclassical approximation.[19] It was obtained by a solution of Poisson's equation, neglecting all quantization effects other than those embodied in the Fermi-Dirac distribution function. Also shown are the experimental values of L_c, the effective-charge distance, as obtained by the two methods (circles and empty squares). Note that for strong accumulation layers, L_c becomes as small as 10 Å. The solid curve labeled L_c has been derived from the theoretical ΔN vs V_s curve by the use of Eq. (21).

V. DISCUSSION

The pulse techniques developed here, combined with the excellent blocking characteristics of the ZnO-electrolyte interface, enabled us to attain extremely strong accumulation layers. The range of surface electron density ΔN investigated (between 10^{13} to 10^{14} cm^{-2})is more than one order of magnitude higher than that encountered on silicon MOS structures. In fact, to the best of our knowledge, this is the first time that accumulation layers with a surface-electron density of 10^{14} cm^{-2} are reported.

There are no published theoretical calculations available for the range of ΔN dealt with in this paper. In addition, because of the material parameters which enter into the theory (ϵ_{sc}, m^*), the calculations cannot be generalized and each calculation is specific to the material considered. Two important corrections were introduced in our calculations. One, the wave-function penetration into the electrolyte and two, the energy correction due to the exchange interaction. Both of these corrections reduce (for different reasons) the magnitude of the potential barrier V_s and the effective charge distance L_c at any given value of ΔN. The penetration of the wave function into the electrolyte increases the effective range of the wave function and thus reduces the energy of the subband E_i. The exchange interaction, on the other hand, reduces the energy of the system because it decreases the probability of two electrons approaching each other very closely.

Apart from the experimental point of view, the choice of ZnO for our experiments was fortunate also from the theoretical point of view. To appreciate this one has to consider the fact that our self-consistent calculations were made without any adjustable parameters. The effective mass has been taken as isotropic and constant (apart from the correction due to the exchange interaction) over the entire V_s range investigated. (This is known to be the case[10] only for the bottom of the conduction band.) The magnitude of the errors in the calculations caused by the different approximations used which neglected the correlation energy and the fluctuations in the potential parallel to the surface is not clear and more theoretical work has to be done to estimate it. However, assuming that these errors are small the agreement between theory and experiment indicates that the ZnO conduction band is indeed spherical up to at least 2 eV above the bottom of the band. This kind of behavior was predicted by band-structure calculations[20] but never, to our knowledge, proved experimentally. Indeed for other materials[18] the departure from parabolity of the conduction band at high energies is evident in the ΔN vs V_s curve. Theoretical calculations for this case were made by Ohkawa and Uemura.[21]

As expected the experimental data in Fig. 7 do not follow the semiclassical curve (long-dashed), except at low values of the barrier height V_s. The semiclassical approximation is meaningful only when the separation between the subbands is less than k_BT or ΔE, the energy broadening due to collision. ΔE is given by $\hbar/\tau$, where τ is the collision time which can be estimated from the mobility. If we take the bulk value of the mobility (about 100 $cm^2/V\,sec$) we obtain $\Delta E \approx 40$ meV, while the room-temperature value of k_BT is about 25 meV. Thus both energies are small compared with the separation of the subbands over most of the range studied ($\Delta N \gtrsim 10^{12}$ cm^{-2}).

The corrections due to the exchange interaction and the wave-function penetration into the electrolyte are not severe (less than 20%) but sufficiently important to be incorporated in our calculations. Small as the difference is between the uncorrected (short-dashed) and corrected (full-line) curves, it is seen that at low ΔN values the experimental points are closer to the former curve while for high ΔN values they definitely follow the latter. The behavior at low ΔN values is as expected because in this range the $T=0$ approximation used is not valid. Consequently, the exchange correction was overestimated (the correction due to wave-function penetration is still negligible). For the high ΔN range, on the other hand, the $T=0$ approximation is very good and there is indeed good agreement with the corrected, "improved self-consistent" curve. The voltage drop across the Helmholtz double layer in the electrolyte could, in principle, affect our results. The exact width

of this layer is not known very well but from the high capacitances obtained in metal-electrolyte systems one can estimate it to be less than 1 Å. Thus it cannot be appreciable compared to the widths of our accumulation layers, which are not narrower than 10 Å.

In conclusion, then, this relatively simple experiment provided very basic information on the properties and quantization of quasi-two-dimensional electronic gas, on the one hand, and on the ZnO band structure on the other hand.

ACKNOWLEDGMENTS

We wish to thank A. Many and H. Gutfreund for helpful discussions and S. Trokman for making available his data to us prior to publication. This work was initially supported by a grant from the United States–Israel Bi-national Science Foundation (BSF, Jerusalem, Israel) and subsequently by a grant from the National Council for Research and Development, Israel and the KFK (Kernforschungszentrum Karlsruhe GmbH), Germany.

[1]D. Eger, Y. Goldstein, and A. Many, Phys. Lett. A 55, 197 (1975).
[2]D. Eger, Y. Goldstein, and A. Many, Surf. Sci. 58, 18 (1976).
[3]A. Rose, *Concepts in Photoconductivity and Allied Problems* (Interscience, New York, 1963).
[4]S. R. Morrison, in *Progress in Surface Science*, edited by S. G. Davison (Pergamon, Oxford, 1971), Vol. 1, p. 105.
[5]J. F. Dewald, Bell Syst. Tech. J. 39, 615 (1960).
[6]A. Many, Y. Goldstein, and N. B. Grover, *Semiconductor Surfaces* (North-Holland, Amsterdam, 1965), Chap. 4.
[7]F. Stern, CRC Crit. Rev. Solid State Sci. 4, 499 (1974).
[8]C. B. Duke, Phys. Rev. 159, 632 (1967); B. Daniel and C. B. Duke, Phys. Rev. 152, 683 (1966); see Eq. (2.2).
[9]J. A. Pals, Phys. Lett. A 39, 101 (1972).
[10]W. Baer, Phys. Rev. 154, 785 (1967).
[11]F. Stern, Phys. Rev. B 5, 4891 (1972).
[12]J. Lauer and T. S. Jayadevaiah, Solid State Electron. 16, 644 (1973).
[13]*American Institute of Physics Handbook, 2nd edition*, edited by D. E. Gray (McGraw-Hill, New York, 1963), pp. 9–51.
[14]F. Stern, J. Comput. Physics 6, 56 (1970).
[15]M. Jonson, J. Phys. C 9, 3055 (1976).
[16]B. Vinter, Phys. Rev. B 15, 3947 (1977).
[17]F. Stern, Japan J. Appl. Phys. Suppl. 2, Pt. 2, 323 (1974).
[18]S. Trokman and A. Many (unpublished).
[19]A. Many, in *Surface Science* (IAEA, Vienna, 1975), Vol. 1, p. 447.
[20]W. Roessler, Phys. Rev. 184, 733 (1969).
[21]F. Y. Ohkawa and Y. Uemura, J. Phys. Soc. Jpn. 37, 1325 (1974).